*remote sensing*

MDPI

*Article*

# Impact of Elevation-Dependent Warming on Runoff Changes in the Headwater Region of Urumqi River Basin

**Zhouyao Zheng [1,2,3,4], Sheng Hong [1,2,3,4], Haijun Deng [1,2,3,4,*], Zhongqin Li [5], Shuang Jin [5,6], Xingwei Chen [1,2,3,4], Lu Gao [1,2,3,4], Ying Chen [1,2,3,4], Meibing Liu [1,2,3,4] and Pingping Luo [7]**

1 College of Geographical Sciences, Fujian Normal University, Fuzhou 350007, China; qsx20201048@student.fjnu.edu.cn (Z.Z.); qsx20211057@student.fjnu.edu.cn (S.H.); cxwchen215@163.com (X.C.); l.gao@foxmail.com (L.G.); chenying_nju@163.com (Y.C.); lmb_18@163.com (M.L.)
2 Fujian Provincial Engineering Research Centre for Monitoring and Assessing Terrestrial Disasters, Fuzhou 350007, China
3 State Key Laboratory for Subtropical Mountain Ecology of the Ministry of Science and Technology and Fujian Province, Fujian Normal University, Fuzhou 350007, China
4 Fujian Provincial Key Laboratory for Plant Eco-Physiology, Fujian Normal University, Fuzhou 350007, China
5 State Key Laboratory of Cryospheric Science, Tien Shan Glaciological Station, Northwest Institute of Eco-Environment and Resources, Chinese Academy of Sciences, Lanzhou 730000, China; lizq@lzb.ac.cn (Z.L.); jinshuang@lzb.ac.cn (S.J.)
6 Chinese Antarctic Center of Surveying and Mapping, Wuhan University, 129 Luoyu Road, Wuhan 430079, China
7 School of Water and Environment, Chang'an University, Xi'an 710000, China; lpp@chd.edu.cn
* Correspondence: denghj@fjnu.edu.cn

**Abstract:** Warming in mountainous areas has obvious elevation dependence (warming rate increases with elevation), which deeply impacts runoff change in mountainous areas. This study analysed the influence of elevation-dependent warming on runoff in the headwater region of the Urumqi River Basin (URB) based on meteorological data, remote sensing images, and runoff data. Results indicated a significant warming rate in the URB from 1960 to 2019 (0.362 °C/decade; $p < 0.01$). The temperature increased with an obvious elevation-dependent warming in the URB, especially during winter. Glaciers sharply retreated in the headwater region of the URB under regional warming, and remote-based results showed that glacier areas decreased by 29.45 km$^2$ (−57.81%) from the 1960s to 2017. The response of glacier mass balance and meltwater runoff to temperature change has a lag of 3 years in the headwater region of the URB. The elevation-dependent warming of temperature changes significantly impacted glacial meltwater runoff in the URB ($R^2 = 0.49$). Rising temperatures altered the glacial meltwater runoff, and the maximum annual runoff of the Urumqi Glacier No. 1 meltwater runoff increased 78.6% in 1990–2017 compared to 1960–1990. During the period of 1960–1996, the total glacial meltwater runoff amounted to 26.9 × 10$^8$ m$^3$, accounting for 33.4% of the total runoff during this period, whereas the total glacial meltwater runoff accounted for 51.1% of the total runoff in 1996–2006. Therefore, these results provide a useful reference for exploring runoff changes in mountainous watersheds in the context of elevation-dependent warming.

**Keywords:** climate change; elevation-dependent warming; glacial mass balance; runoff; Urumqi River Basin



**Citation:** Zheng, Z.; Hong, S.; Deng, H.; Li, Z.; Jin, S.; Chen, X.; Gao, L.; Chen, Y.; Liu, M.; Luo, P. Impact of Elevation-Dependent Warming on Runoff Changes in the Headwater Region of Urumqi River Basin. *Remote Sens.* **2022**, *14*, 1780. https://doi.org/10.3390/rs14081780

Academic Editor: Gareth Rees

Received: 23 February 2022
Accepted: 5 April 2022
Published: 7 April 2022



## 1. Introduction

According to the Fifth Intergovernmental Panel on Climate Change (IPCC) report, global mean temperature has risen by 0.85 °C (0.65–1.06 °C) from 1880 to 2012, which is faster than any 50-year warming rate in the last 200 years, and this warming trend is expected to continue [1]. Mountain systems are extremely sensitive to climate change, and the warming context is characterized by accelerated glacier melt in mountainous areas [2], reduced seasonal snowpack [3], permafrost degradation [4], and larger runoff

variability coefficients [5], which not only trigger imbalances in mountain ecosystems but also stimulate conflicts over the co-requirements of water resources in the course of regional socioeconomic development.

Mountain areas are an important part of the surface critical zone, providing habitat for approximately 33% of terrestrial biodiversity, and solid water resources such as snow and ice are abundant and provide more than 50% of the world's freshwater [6]. Changes in mountain climate hydrological processes in the context of global warming are manifested by changes in precipitation forms, from snowfall to rainfall [7], a reduction in multiyear snowpack [8], accelerated glacier ablation [9], and significant intra- and interannual changes in mountain runoff [10]. Therefore, a comprehensive and systematic understanding of the climatic and hydrological processes in mountainous regions under global warming is of great importance [11].

Current research results have shown that there is an evident elevation-dependent characteristic of warming changes in mountain areas, called elevation-dependent warming (EDW) [12], which is a distinctive feature of the response of mountain climate change to global warming. For example, warming rates in the tropical Andes were in the range of 0.10–0.11 °C/decade ($p < 0.05$) from 1939 to 1998 [13]. The elevation dependence of warming is significant in the alpine region, with a correlation of 0.83 between temperature change and elevation change [14]. Temperature change in the Rocky Mountains has a clear EDW phenomenon and is strongly influenced by the season [15]. In addition, the rate of elevational warming in the Saint Elias Mountains increased from 1979 to 2016, with an average rate of surface warming at 5500–6000 m above sea level of 0.028 ± 0.013 °C/a, which is 1.5 times the surface warming rate between 2000 and 2500 m during the same period [16]. The warming trend has reached 0.04 °C/yr in the Tibetan Plateau [17], which is much faster than the surrounding areas and shows obvious elevation-dependent warming. This elevation-dependent warming will continue [18], which will have far-reaching effects on the cryosphere system, ecosystem, and climate and hydrological systems of the Tibetan Plateau. The warming rates of mean, maximum, and minimum temperatures in the Tian Shan have all accelerated with increasing elevation [19], and the EDW phenomenon is particularly pronounced in the Tian Shan [20].

Driven by the altitudinal dependence of warming, glaciers in the High Asia region are showing an accelerated retreating trend, which has caused great concern to the community [21]. Over the last half-century, glaciers have been in a state of general retreat in China [22], which shows a reduction of 7625 $km^2$ (15%) in glacier area and 0.9–1.3 × $10^3$ $km^3$ (20–28%) in ice reserves. Increase in glacier meltwater runoff due to glacier retreat was estimated to be more than 5.5%. Glacial retreat of the No. 1 glacier in the URB from 1960 to 1993 was caused by increasing temperatures and decreasing precipitation [23].

The No. 1 Glacier of the URB is one of the longest monitored records and best-documented glaciers worldwide. Numerous studies have been conducted on the No. 1 glacier, such as changes in glacier area and length [24], glacier movement velocity [25], glacier mass balance [26], and glacier runoff response processes to climate change [27]. Based on meteorological data and glacier observations from the Tian Shan glacier station, Li et al. [24] found that the source area of the URB has been in a significantly warm and wet phase since the mid-20th century, and that the area of the Urumqi River No. 1 glacier showed an accelerated retreat from 1962 to 2000. Thus, glaciers retreating in the MRB has altered surface albedo and accelerated warming in high-elevation regions, exacerbating the elevation dependence of warming, which in turn accelerates regional snow and glacier melting and changes intra- and interannual variability in basin runoff. However, there is a lack of attention to runoff changes in the context of the elevation dependence of warming.

Therefore, in this study, we focus on the influences of elevation-dependent warming on runoff changes in the headwater region of the URB from the 1960s to 2017. Section 2 presents the study area, data sources, and methodology. Section 3 focuses on the effects of

warming on runoff in the URB. Section 4 provides a discussion, and Section 5 concludes the study.

## 2. Data and Methods

### *2.1. Study Area*

The Urumqi River originates from Glacier No. 1 near the Tiangeer II peak in the Tian Shan Mountains, and the entire basin spans the alpine cold zone, subalpine zone, middle mountain zone, and low mountain hilly zone [28], making it a typical inland river basin in the arid region of northwest China (Figure 1). The basin area is 1088.31 km$^2$. The high mountainous area of the URB is an area of glacial ice margin action, with modern glaciers and ice erosion and ice accretion landforms developing throughout the region. Urumqi city, downstream of the URB, is the socioeconomic centre of Xinjiang, and the Urumqi River is its main water supply source. The Urumqi River supports agricultural, industrial, domestic, and ecological environmental water consumption, accounting for 62%, 12%, 23%, and 4%, respectively [29]. Future changes in climate and water resources in the URB will have an important impact on water resource assurance and ecological environmental protection for the socioeconomic development of the region [30]. In this study, the whole URB is divided into six elevation ranges, namely, ≤2000 m, 2000–2500 m, 2500–3000 m, 3000–3500 m, 3500–4000 m, and >4000 m, to analyze the warming change characteristics of different elevation bands.

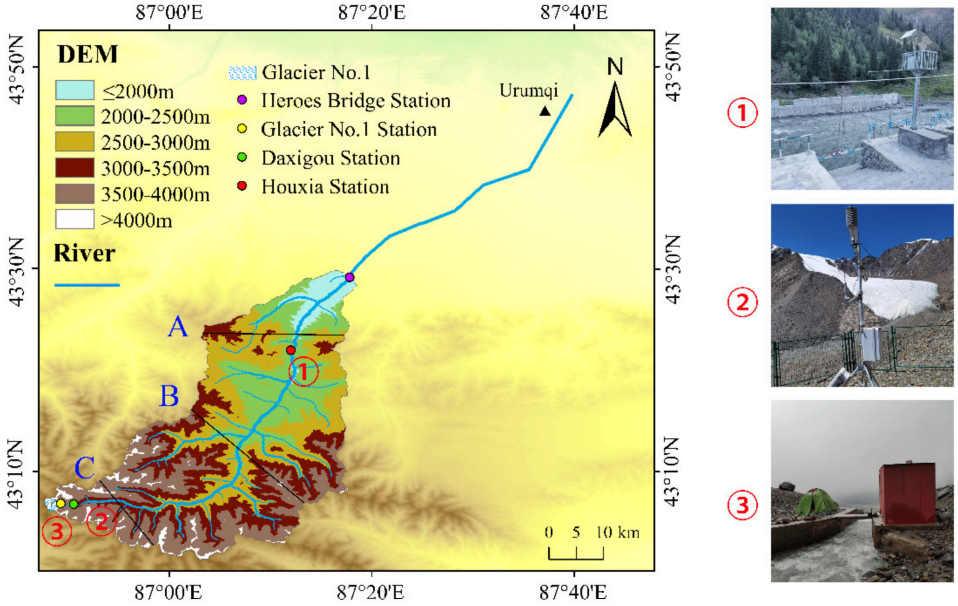


**Figure 1.** The Urumqi River Basin. ①, ②, and ③ are the Houxia hydrological station, Daxigou meteorology station, and Glacier No. 1 hydrological station, respectively. Lines A, B, and C show the topography and temperature profiles in Figure 5. The glaciers boundary shape format data are from the second glacier inventory data, and DEM elevation data are from the SRTM (https://earthexplorer.usgs.gov/, accessed on 4 April 2022).

### *2.2. Data Sources*

#### 2.2.1. Landsat Images

Glacier boundary data since 1991 were extracted by decoding Landsat images data. The Landsat remote sensing image data were provided by the United States Geological Survey (USGS; https://earthexplorer.usgs.gov/, accessed on 4 April 2022) and the Geospatial Data Cloud (http://www.gscloud.cn/search, accessed on 4 April 2022). The data are radiometrically corrected and geometrically corrected products, and the corrected image data are mapped to the specified map projection coordinates.

To improve the accuracy of glacier interpretation, we followed two principles in the process of image selection: (1) we selected remote sensing images at the end of the glacier melting period from July to September in summer, when the glacier area is less affected by snow, and (2) we selected images with no or few clouds. For some images with more clouds, although the whole image contains high cloud content, the glacier area is less affected and could also be selected. In addition, images from the same area and different time periods (2 years before and after) and the data of the second glacier inventory of China were chosen to assist in the comparative interpretation of this study so that the effects of seasonal snow and clouds could be removed to the greatest extent possible. The final remote sensing imagery selected are shown in Table 1.

**Table 1.** Basic information of the remote sensing images used in this study.

| Year | Sensors | Obtaining Data | Cloudiness (%) | Resolution (m) | Image Information | Reference Image |
|---|---|---|---|---|---|---|
| 1991 | TM | 1 September 1991 | 1 | 30 | LT51430301991244BJC01 | 29 August 1996 |
| 1996 | TM | 29 August 1996 | 0 | 30 | LT51430301996242ISP00 | 28 July 1996 |
| 2001 | TM | 10 July 2001 | 12 | 30 | LT51430302001191BJC00 | 28 July 1996 |
| 2002 | TM | 15 September 2002 | 21 | 30 | LT51430302002258BJC01 | 14 August 2002 |
| 2003 | TM | 17 August 2003 | 1 | 30 | LT51430302003229BJC00 | 15 September 2002 |
| 2004 | TM | 2 July 2004 | 11 | 30 | LT51430302004184BJC00 | 17 August 2003 |
| 2005 | TM | 7 September 2005 | 1 | 30 | LT51430302005250BJC00 | 2 July 2004 |
| 2006 | ETM | 1 August 2006 | 2 | 30/15 | LE71430302006213ASN00 | 7 September 2005 |
| 2008 | TM | 30 August 2008 | 21 | 30 | LT51430302008243BJC00 | 1 August 2006 |
| 2009 | ETM | 25 August 2009 | 1 | 30/15 | LE71430302009237ASN00 | 30 August 2008 |
| 2010 | TM | 20 August 2010<br>4 August 2010 | 1<br>8 | 30<br>30 | LT51430302010232IKR00<br>LT51430302010216IKR00 | 30 August 2008 |
| 2011 | TM | 23 August 2011 | 0 | 30 | LT51430302011235KHC01 | 20 August 2010 |
| 2012 | ETM | 2 September 2012 | 0 | 30/15 | LE71430302012246PFS00 | 23 August 2011 |
| 2013 | OLI_TIRS | 28 August 2013<br>27 July 2013 | 1.22<br>6.31 | 30/15<br>30/15 | LC81430302013240LGN01<br>LC81430302013208LGN01 | 2 September 2012 |
| 2014 | OLI_TIRS | 31 August 2014 | 1.32 | 30/15 | LC81430302014243LGN01 | 28 August 2013 |
| 2015 | OLI_TIRS | 18 August 2015 | 1.76 | 30/15 | LC81430302015230LGN01 | 31 August 2014 |
| 2016 | OLI_TIRS | 4 August 2016 | 1.72 | 30/15 | LC81430302016217LGN02 | 18 August 2015 |
| 2017 | OLI_TIRS | 22 July 2017 | 1.24 | 30/15 | LC81430302017203LGN00 | 4 August 2016 |

The digital elevation data are mainly used to assist in the geometric correction of remote sensing imagery and the extraction of elevation for the study area. The Shuttle Radar Topography Mission (SRTM) digital elevation data used in this study have a spatial resolution of 30 m. This dataset was produced by NASA and the National Imagery and Mapping Agency (NIMA) of the Department of Defense using SRTM data collected by the U.S. Space Shuttle Endeavour on 11 February 2000. The radar image data were produced using the SRTM system onboard the space shuttle Endeavour on 11 February 2000, covering a range of 60° north and south latitude.

#### 2.2.2. Glacier Inventory Data

The glacier inventory data are from the first glacier inventory and the second glacier inventory of China conducted by the Lanzhou Institute of Glacial Permafrost, Chinese Academy of Sciences, in accordance with international glacier inventory standards.

#### 2.2.3. Temperature Data

Temperature data were obtained using the 1 km resolution monthly average temperature dataset for China in 1960–2017 from the National Science and Technology Infrastructure Platform—National Data Centre for Earth System Science (http://www.geodata.cn, accessed on 4 April 2022) with a spatial resolution of 0.0083333° (approximately 1 km). In this study, the monthly temperature data of the Daxigou meteorological station in the headwater region of the URB were compared with the grid data corresponding to the station.

The results show that there is an underestimation of the grid data in the temperature range less than 0 °C, and the lower the temperature is, the more serious the underestimation. In the temperature range greater than 0 °C, the grid data and the observation data are very close, basically along the diagonal ($y = x$) distribution. On the whole, the determination coefficient $R^2 = 0.98$, indicating that this set of data has good applicability in the headwater region of the URB (Figure 2), which can be used to analyze the temperature change characteristics.

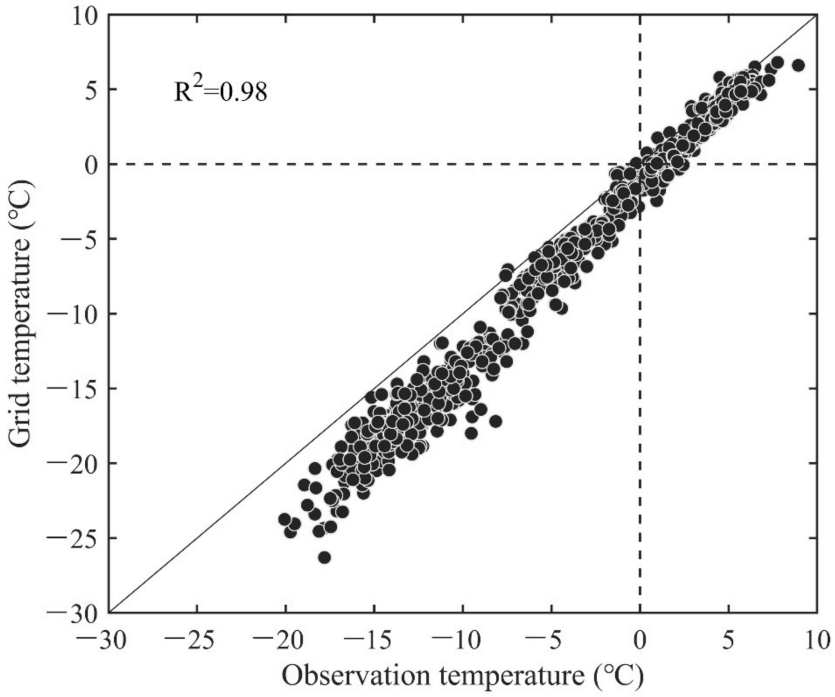


**Figure 2.** Scatter plot of the monthly mean temperature of meteorological station observations from the Daxigou station compared to the monthly mean temperature at the corresponding grid point, with the black dashed line indicating that the temperature is equal to 0 °C.

#### 2.2.4. Glacier Mass Balance Data

The Glacier No. 1 mass balance data in the URB are provided by the world glacier monitoring service centre (https://wgms.ch/, accessed on 4 April 2022). The center collected standardized observation data and glacier inventory of glacier mass, volume, area, and length (glacier fluctuation) changing with time and provided basic data of glacier mass balance.

#### 2.2.5. Runoff Data

The glacier meltwater runoff data for Glacier No. 1 of the URB come from the relevant literature [31], and the year range is 1960–2017. The runoff of the outlet in the headwater region of the URB is from the Hero Bridge hydrological station provided by the hydrological bureau of the Xinjiang Uygur Autonomous Region. The selected period is 1960–2007 because of the interference of building the Hero Bridge reservoir after 2007.

### *2.3. Methods*

#### 2.3.1. Extent of Glacier Extraction

First, based on ENVI 5.1 software, the Landsat satellite image was corrected by system radiation. The remote sensing image was then fixed by the geometric correction of ground control points through DEM. Referring to the relevant literature, a simple test comparison of supervised classification, unsupervised classification, and the ratio threshold method was carried out [32,33]. The ratio threshold method combined with the visual interpretation

method was selected to extract the glacier boundary [34]. The ratio threshold method calculates the ratio of band 3 to band 5 (TM3/TM5) based on ENVI 5.1 software to obtain the ratio image. On this basis, based on ArcGIS10.2 software, combined with the second glacier catalogue data and DEM data, the glacier was visually interpreted and identified, and the glacier range boundary was extracted and then converted into shape format. Finally, the remote sensing images in different periods were compared to correct the glacier boundary. The advantage of this method is that it can improve the accuracy of glacier extraction, reduce the error, and effectively avoid the influence of clouds and snow.

Errors arising from processes such as remote sensing image correction can be calculated by Equation (1). The formula for calculating the accuracy of glacier length change typically uses the root mean square error, which is given by [35]

$$E = \sqrt{\delta^2 + \varepsilon^2} \quad (1)$$

where $E$ is the length change error, $\delta$ is the resolution of the previous period of remote sensing images, and $\varepsilon$ is the resolution of the later period of remote sensing images.

The error in the change in glacier area was calculated using the formula for the uncertainty in the change in area and length, which is given by

$$a = A \cdot (2E/x) \quad (2)$$

where $a$ is the area change error, $A = x^2$, $x$ is the resolution of the remote sensing image.

In this study, the spatial resolution of the remote sensing images is 30 m (Landsat TM) and 15 m (Landsat OLI_TIRS). Based on Equations (1) and (2), the error in length change for the area from 1991–2011 and 2011–2017 can be calculated as 33.5 m and 21.2 m, respectively; the error in the area is 0.002 $km^2$ and 0.001 $km^2$, not exceeding 0.01 $km^2$.

#### 2.3.2. Estimates of Glacial Storage Volume

The estimation of glacier storage is based on empirical Equation (3) obtained by Liu et al. [36]:

$$V = 0.04S^{1.35} \quad (3)$$

where $S$ is the glacier area ($km^2$) and $V$ is the glacier ice storage volume ($km^3$).

The glacier meltwater runoff in the URB is obtained by calculating the glacier storage and loss at different periods.

#### 2.3.3. Mann–Kendall Nonparametric Tests

The Mann–Kendall (M–K) test sample does not need to follow a certain distribution and is not disturbed by a few outliers. It is widely used in the analysis of climatic parameters and hydrological series [37]. In this study, the M–K trend test was used to assess the trends in temperature, glacial material balance, and runoff. The trend slope was estimated using Sen's estimation [38]. In addition, the M–K abrupt test was used to detect the abrupt points of temperature, glacier mass balance, and runoff.

## 3. Results

### *3.1. Temperature Change*

The average annual temperature is −2.72 °C in the headwater region of the URB from 1960 to 2017. The lowest temperature appeared in 1969 at −4.61 °C, and the highest temperature in 2007 at −1.34 °C (Figure 3). The temperature change shows a significant upwards trend, with a warming rate of 0.362 °C/decade ($p < 0.01$). This value is much higher than the global average temperature changes (0.23 °C/decade) during the same period [39]. The average temperature in 1990–2017 was 1.13 °C warmer than that in 1960–1989. The warming rate of the mean temperature increases with elevation (Table 2); therefore, there is an elevation-dependent warming phenomenon in the URB.

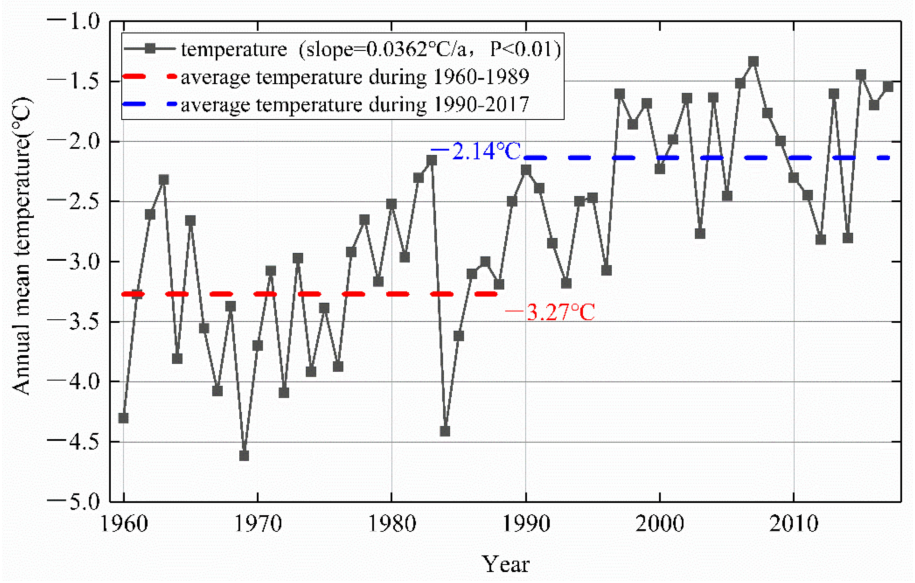


**Figure 3.** Average annual temperature in the headwater region of the Urumqi River Basin.

**Table 2.** Temperature variation in different elevation zones in the headwater region of the URB.

| Elevation Zone | Mean (°C) | Std | Trend (°C/Decade) | *p*-Value |
|---|---|---|---|---|
| ≤2000 m | 2.91 | 0.824 | 0.357 | ** |
| 2000–2500 m | 1.31 | 0.827 | 0.360 | ** |
| 2500–3000 m | −1.13 | 0.825 | 0.361 | ** |
| 3000–3500 m | −4.34 | 0.823 | 0.362 | ** |
| 3500–4000 m | −6.78 | 0.824 | 0.363 | ** |
| >4000 m | −8.50 | 0.822 | 0.362 | ** |
| Study region | −2.72 | 0.824 | 0.362 | ** |

Note: "**" indicates that the results passed the significance test at the 0.01 confidence level ($p < 0.01$).

At the same time, there is significant seasonal variation in the elevation-dependent warming of temperature change in the headwater region of the URB. The changes in the annual mean temperature show a more obvious elevation-dependent warming (Figure 4a), in which 3500–4000 m is the elevation band with the largest warming rate, reaching 0.363 °C/decade. In spring, the warming rate of temperature had no obvious elevation-dependent warming (Figure 4b). In summer, the warming rate increases below 3500 m, from 0.280 °C/decade to 0.285 °C/decade, reaching a maximum at 3000–3500 m. The warming rate slows down at elevations above 4000 m, but overall, the rate of temperature change in summer tends to increase with elevation (Figure 4c). In autumn, the rate of warming is significantly elevation-dependent, rising from 0.273 °C/decade at ≤2000 m to 0.286 °C/decade near 3000 m, reaching a maximum of 0.287 °C/decade at 4000 m (Figure 4d). In winter, the rate of warming increases with elevation, reaching a maximum of approximately 0.456 °C/decade near 3500 m above sea level before slowing down (Figure 4e).

Overall, significant warming has occurred in the headwater region of the URB since 1960, with the highest warming rate in winter (0.45 °C/decade), followed by spring, with the lowest warming rates in summer and autumn. In addition, the warming rate increases with elevation, i.e., showing obvious elevation-dependent warming. It can be seen that there is a consistency between the topographic relief and the average annual temperature change rate (Figure 5). The elevation-dependent warming in the basin will have positive feedback on glacier changes, for example, accelerating glacier ablation.

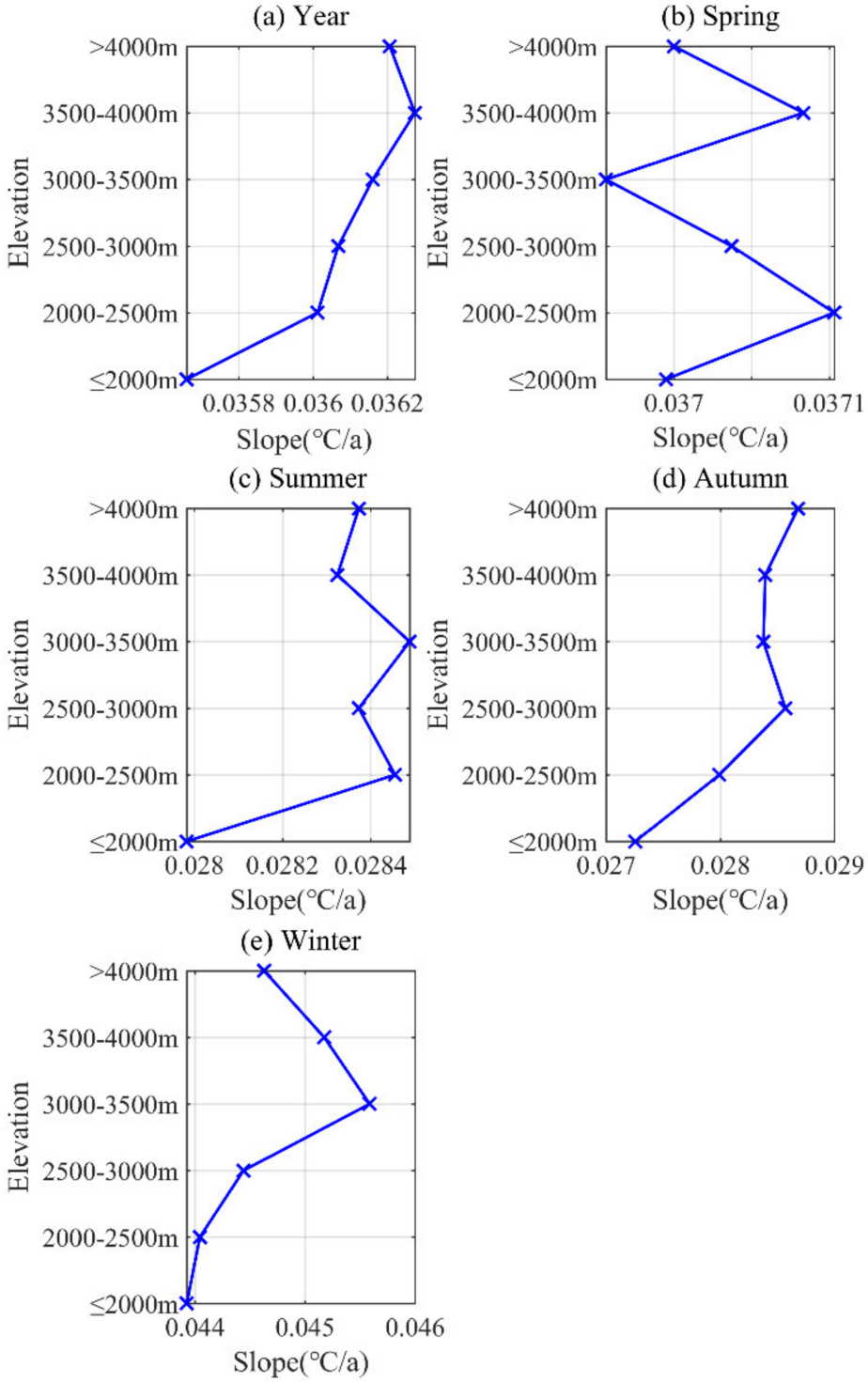


**Figure 4.** Elevation change of warming in the headwater region of the URB from 1960 to 2017; (**a**) annual average, (**b**) spring, (**c**) summer, (**d**) autumn, (**e**) winter.

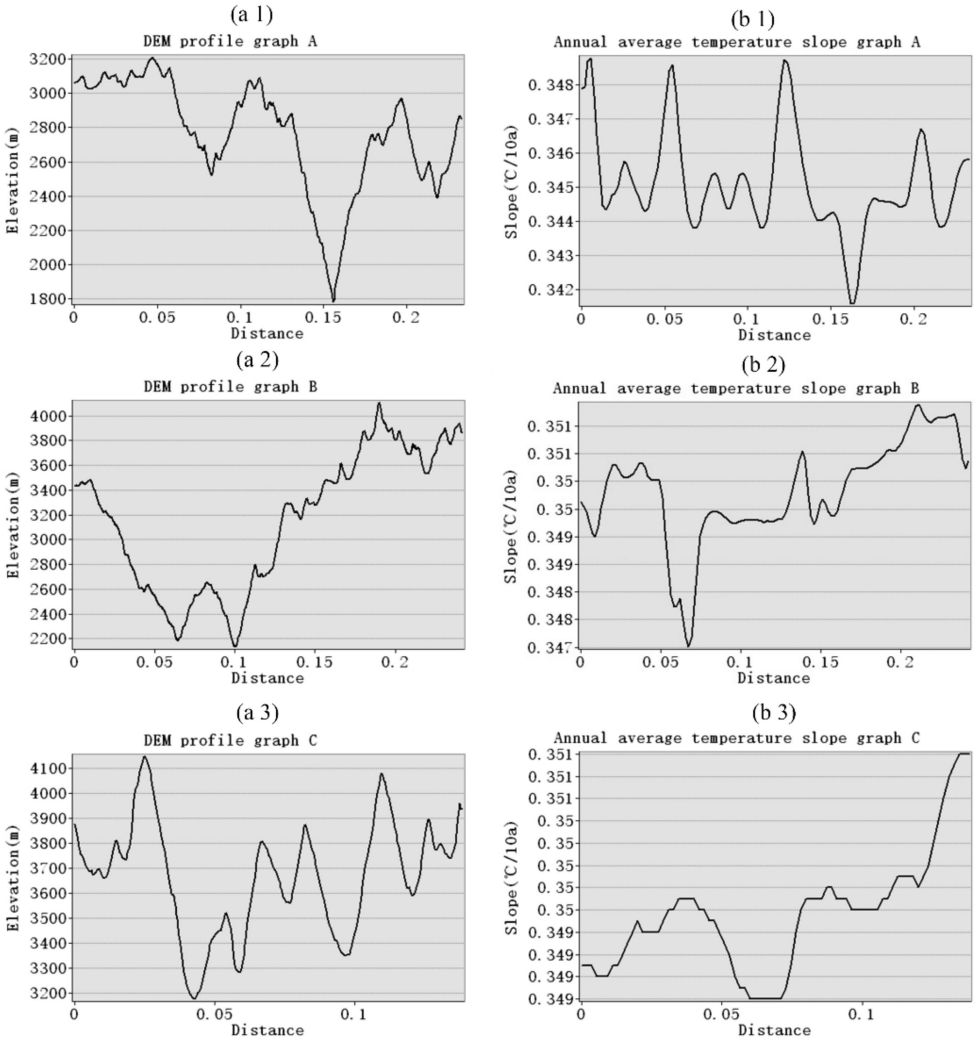


**Figure 5.** Comparison of topographic profiles and mean annual warming rate profiles: (**a1**) Line A topographic profile, (**a2**) Line B topographic profile, (**a3**) Line C topographic profile, (**b1**) Line A mean annual warming rate profile, (**b2**) Line B mean annual warming rate profile, (**b3**) Line C mean annual warming rate profile.

### *3.2. Glacial Changes*

#### 3.2.1. Glacier Area Change

All glaciers in the URB are small glaciers in the headwater region because the largest individual glaciers do not exceed 5 km$^2$ in area. A total of 136 glaciers were catalogued in the first glacier inventory of China, 81 glaciers in 1991, 93 glaciers in 2001, 98 glaciers in 2011, and 100 glaciers in 2017; accordingly, the glacier areas were 50.95 km$^2$, 39.33 km$^2$, 35.52 km$^2$, 26.32 km$^2$, and 21.50 km$^2$, respectively. Glacial areas showed a rapid decrease (Figure 6), with retreat rates from 1960s–2017, 1960s–1991, 1991–2001, 2001–2011, and 2011–2017 of 9.97%/10 a, 7.35%/10 a, 9.71%/10 a, 25.90%/10 a, and 30.52%/10 a, respectively. Comparing the number of glaciers, it is seen that the number of glaciers increased in the URB, but this is not due to the creation of new glaciers but to the ablation of large glaciers split into smaller pieces. Thus, the accelerated retreat of glacier areas has been more pronounced in the Urumqi River Basin from 1960 to 2017, especially in the last ten years.

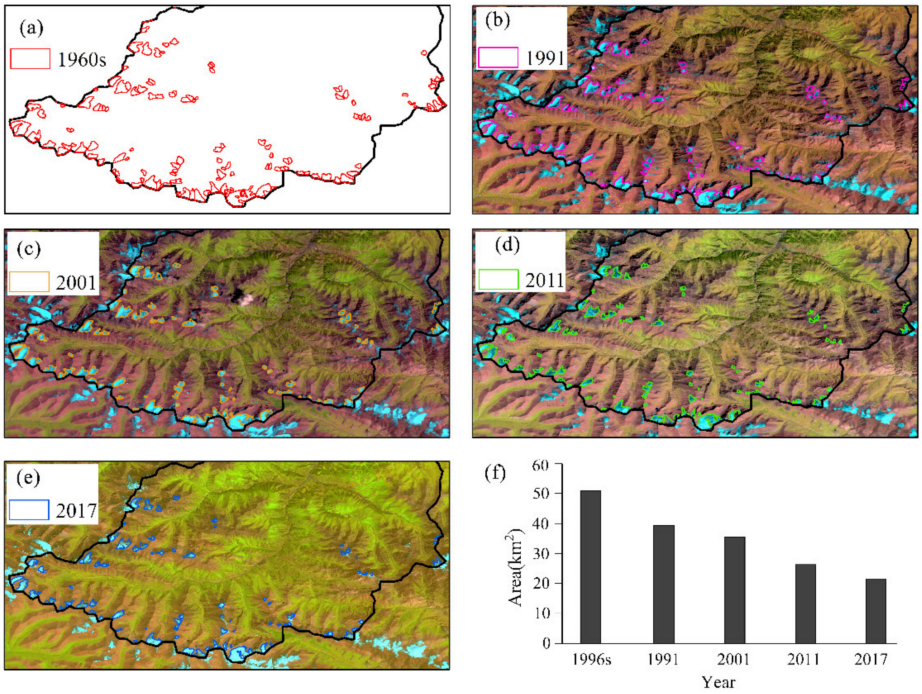


**Figure 6.** Glacier area changes in the URB during different periods. From (**a**–**e**) is glacier boundary in 1960s, 1991, 2001, 2011, and 2017, respectively; (**f**) shows the glacier changes in the URB in different periods. The background images in (**b**–**e**) are corresponding Landsat images.

### 3.2.2. Glacier Area Changes at Different Elevation Zones

The results show that the glacier area is concentrated between 3600 and 4200 m, with the smallest area between 3300 and 3600 m above sea level. The area of glacier distribution increases as the elevation rises and gradually decreases after reaching 3800–3900 m (Figure 7).

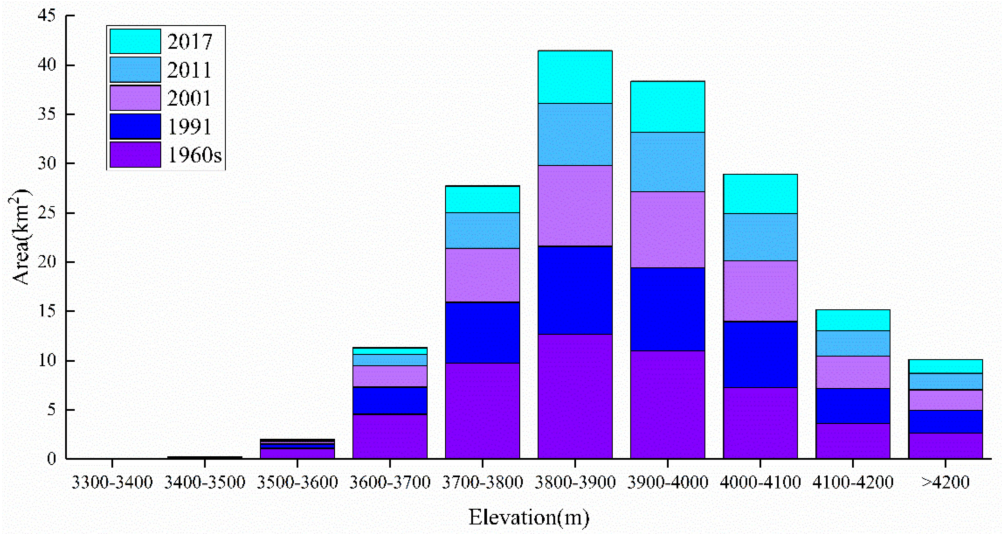


**Figure 7.** Glacier changes at different elevation zones in the headwater region of the URB.

The results in Figure 8a show that glacier areas tend to decrease in all elevation zones. The retreat of glaciers in the URB generally tends to increase and then decrease with elevation; the greatest retreat change was concentrated between 3700 and 3900 m, and the greatest retreat was at 3800–3900 m, reaching −7.34 km$^2$. The rate of glacier changes in the 3300–3500 m range is 100%, indicating that all glaciers in this elevation range have ablated. The rate of glacier change is lowest at 4100–4200 m and tends to increase again at >4200 m

(Figure 8b). Combined with the rate of warming increasing with elevation (Figure 8c), although there was elevation-dependent warming, there was no increase in the glacier retreat rate. This is due to the lower temperatures at higher elevations, and although the rate of warming increases, the overall temperature does not have a high impact on glacier ablation. Overall, there is a close relationship between the rate of warming and the rate of glacier change at the same elevation ($R^2$ = 0.49) (Figure 8d).

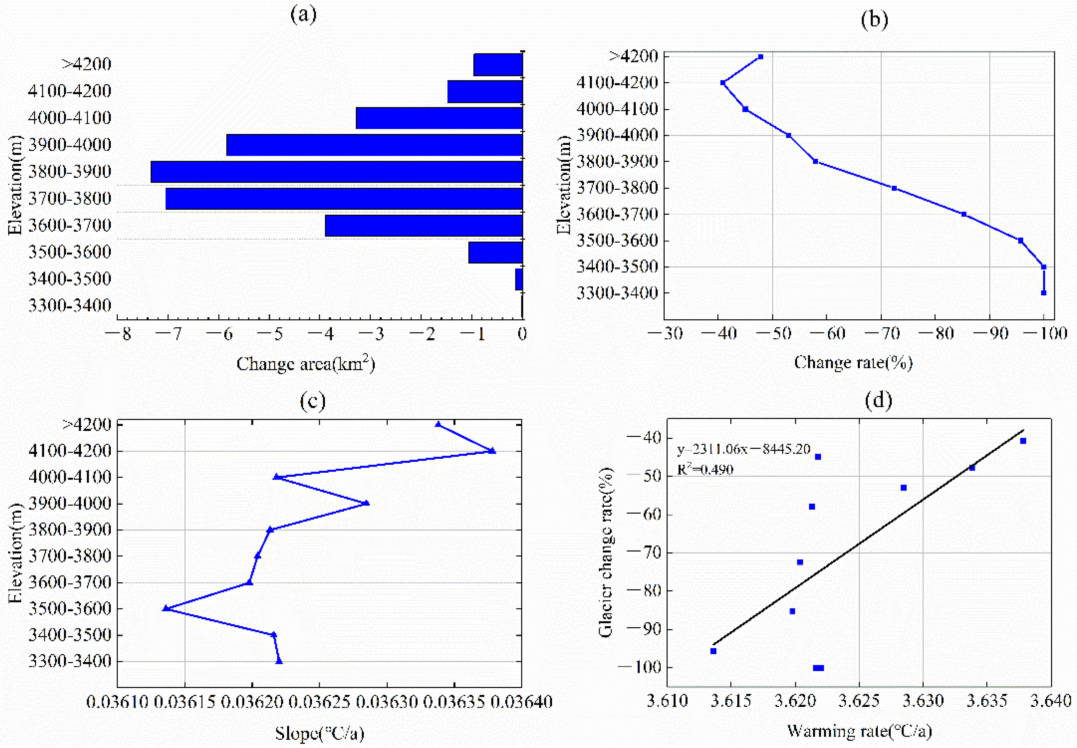


**Figure 8.** Glacier changes at different elevation zones: (**a**) area of glacier change at different elevations, (**b**) rate of glacier change at different elevations, (**c**) rate of warming at different elevations, and (**d**) scatter plot of warming rate vs. rate of glacier change at corresponding elevations.

### *3.3. Runoff Changes in the Headwater Region of the URB*

#### 3.3.1. Changes in Glacial Meltwater Runoff

Rising temperatures are the dominant factor in the change in glacier meltwater runoff in the URB. Table 3 shows that an abrupt change in the annual mean temperature in the URB occurred around 1990, and the annual mean temperature has increased significantly since 1990, with a mean temperature increase of 1.13 °C. An abrupt change in glacier mass balance and glacier meltwater runoff for Urumqi Glacier No. 1 both occurred around 1993. The average annual mass balance for Urumqi Glacier No. 1 from 1960 to 1992 was −141 mm w. e., whereas it reached −597 mm w. e. from 1993 to 2017. Similarly, the average annual meltwater runoff of Urumqi Glacier No. 1 from 1960 to 1992 was 157 $10^4$ $m^3$, whereas it reached 269 $10^4$ $m^3$ from 1993 to 2017, with an increase of 112 $10^4$ $m^3$. Therefore, the response of glacier changes to temperature lags by 3 years in the URB.

**Table 3.** Abrupt changes in temperature, Urumqi Glacier No. 1 mass balance, and glacier meltwater runoff in the URB from 1960 to 2017.

| Variables | Abrupt Years | Mean Value before Abrupt | Mean Value after Abrupt | Difference |
|---|---|---|---|---|
| Average annual temperature (°C) | 1990 | −3.27 | −2.14 | 1.13 |
| Mass balance of Glacier No. 1 (mm w·e) | 1993 | −141 | −597 | −456 |
| Meltwater runoff of glacier No. 1 ($10^4$ $m^3$) | 1993 | 157 | 269 | 112 |

The glacier area in the whole URB decreased sharply, from 50.95 $km^2$ in the 1960s to 21.50 $km^2$ in 2017, a reduction of 57.81% (Table 4). The glacier area in 1991 was 22.8% less than that in the 1960s, in 2006 was 25.6% less than that in 1991, and in 2017 was 45.3% less than that in 1991. According to Equation (3), the glacier storage in the 1960s was 8.07 $km^3$, that in 1991 was 5.69 $km^3$, and that in 2017 was only 2.69 $km^3$ (Table 4). The glacier storage in 1991 decreased by 29.5% compared with that in the 1960s, contributing 23.8 $\times$ $10^8$ $m^3$ runoff from 1960 to 1991. The glacier storage in 2006 decreased by 32.9% compared with that in 1991, which contributed 18.7 $\times$ $10^8$ $m^3$ runoff from 1991 to 2006. Glacier storage in 2017 decreased by 55.8% compared with that in 1991, contributing 31.7 $\times$ $10^8$ $m^3$ runoff from 1991 to 2017.

**Table 4.** Variations in glacier area and storage in the headwater region of the URB from the 1960s to 2017.

| Periods | Area ($km^2$) | Glacier Storage ($km^3$) | Rate of Change Relative to 1960s | | Rate of Change Relative to 1991 | |
|---|---|---|---|---|---|---|
| | | | Area | Glacier Storage | Area | Glacier Storage |
| 1960s [a] | 50.95 | 8.07 | 100% | 100% | - | - |
| 1991 | 39.33 | 5.69 | −22.8% | −29.5% | 100% | 100% |
| 1996 | 37.74 | 5.38 | −25.9% | −33.4% | −4.1% | −5.5% |
| 2001 | 35.52 | 4.96 | −30.3% | −38.6% | −9.7% | −12.9% |
| 2006 | 29.26 | 3.82 | −42.6% | −52.7% | −25.6% | −32.9% |
| 2011 | 26.32 | 3.31 | −48.4% | −59.0% | −33.1% | −41.9% |
| 2017 | 21.50 | 2.52 | −57.8% | −68.8% | −45.3% | −55.8% |

Note: [a] represents the first glacier inventory of China.

The mass balance of Urumqi Glacier No. 1 was in a negative balance state from the 1960s to 2017 (Figure 9). The maximum negative balance occurred in 2010, reaching −1327 mm w. e. The maximum positive mass balance occurred in 1965, which was 374 mm w. e. The cumulative mass balance of Urumqi Glacier No. 1 reached −19,572 mm w. e., which means that Glacier No. 1 became thinner by approximately 19.57 m from the 1960s to 2017.

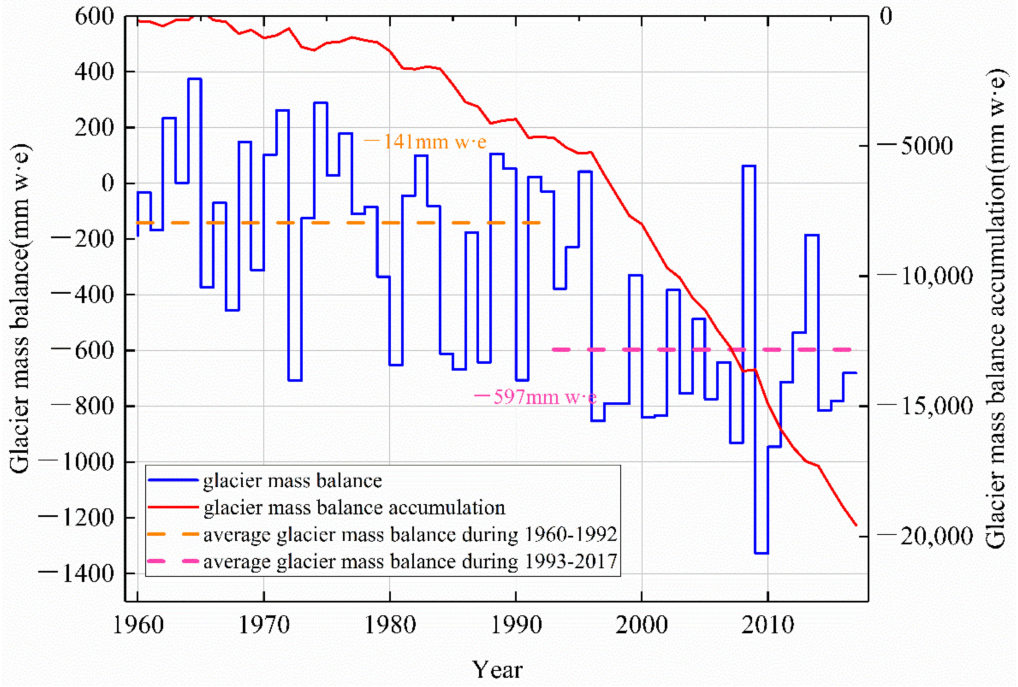


**Figure 9.** Changes in mass balance of Urumqi Glacier No. 1.

The annual glacier meltwater runoff at Urumqi Glacier No. 1 hydrological station shows a slight upwards trend (Figure 10a), with a trend rate of 2.928 $\times$ $10^4$ $m^3$/a. The glacier meltwater runoff changes were relatively stable from 1960 to 1992, with an average

of 1.57 × $10^6$ $m^3$, whereas the glacier meltwater runoff increased from 1993 to 2017, with an average value of up to 2.69 × $10^6$ $m^3$, an increase of 1.12 × $10^6$ $m^3$ in 1993–2017 compared to 1960–1992. The cumulative anomaly of annual runoff in Urumqi Glacier No. 1 shows a relatively stable change from 1960 to 1992, whereas it has rapidly increased since 1993 (Figure 10b). This indicates that the runoff of Glacier No. 1 experienced an obvious abrupt change around 1993.

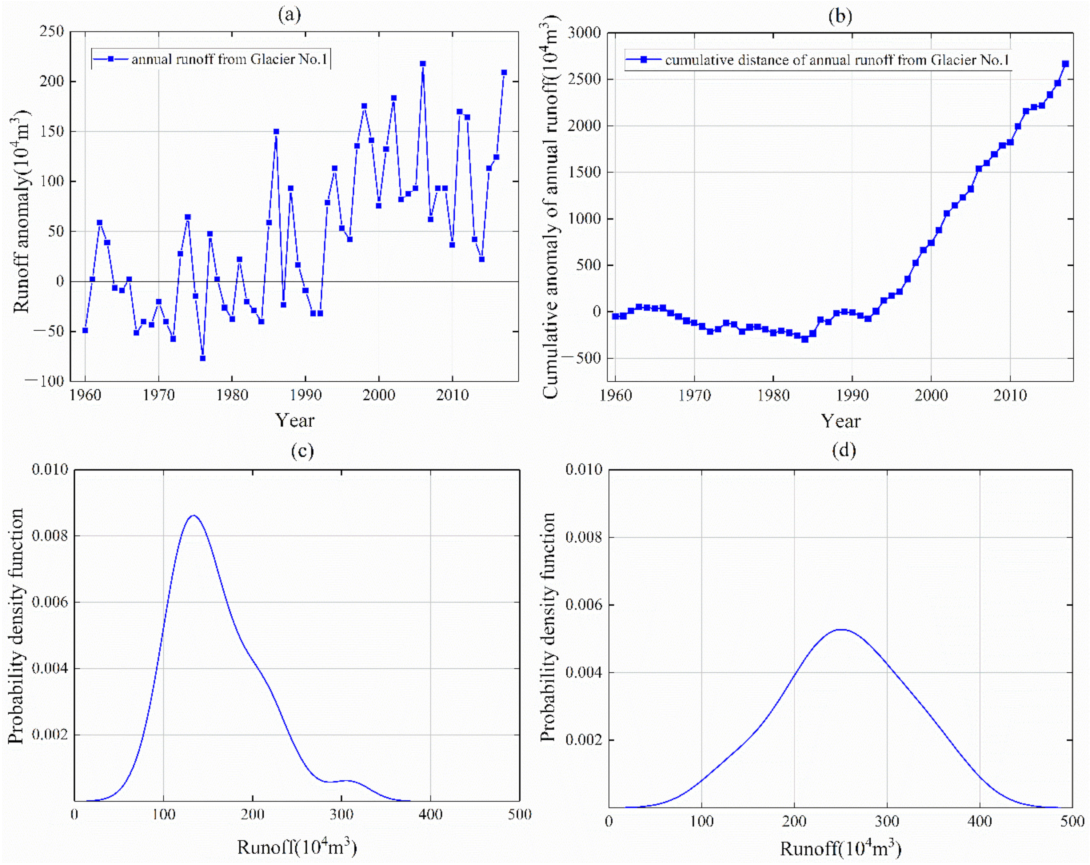


**Figure 10.** Observed runoff from Glacier No. 1 hydrological station at URB; (**a**) annual runoff, (**b**) cumulative anomaly of annual runoff, (**c**) annual runoff probability density from1960 to1989, (**d**) annual runoff probability density from 1990 to 2017.

Rising temperatures altered the maximum annual glacial meltwater runoff. An abrupt change in temperature in the URB occurred around 1990, which accelerated glacier ablation, resulting in an increase in glacial meltwater runoff. The maximum annual runoff of Urumqi Glacier No. 1 was only 1.4 × $10^6$ $m^3$ in 1960–1990 (Figure 10c), whereas it reached 2.5 × $10^6$ $m^3$ in 1990–2017 (Figure 10d), an increase of 78.6%.

### 3.3.2. Total Runoff Changes in the Headwater Region of the URB

The Hero Bridge hydrological station is the outlet of the headwater region of the URB, representing the total runoff. The observation results show a relatively stable (with a slight upwards trend) runoff variation at the Hero Bridge hydrological station from 1960 to 2007. In 2001, the maximum negative runoff anomaly was −5.775 × $10^7$ $m^3$, and the maximum positive runoff anomaly was 1.136 × $10^8$ $m^3$ in 1996 (Figure 11a). The change in total runoff in the headwater region of the URB can be divided into two stages: from 1960 to 1996, runoff showed an increasing trend (5.8 × $10^5$ $m^3$/a), whereas runoff showed a decreasing trend from 1996 to 2007, with a decreasing trend of −4.6 × $10^6$ $m^3$/a. In addition, the results show that the change in the annual runoff anomaly was relatively stable from 1960 to 1990 (Figure 11b), but it has turned into a sharp increase since 1991, probably due to the

increase in glacial meltwater. However, after 2000, the variation in annual runoff became flat again (Figure 11b).

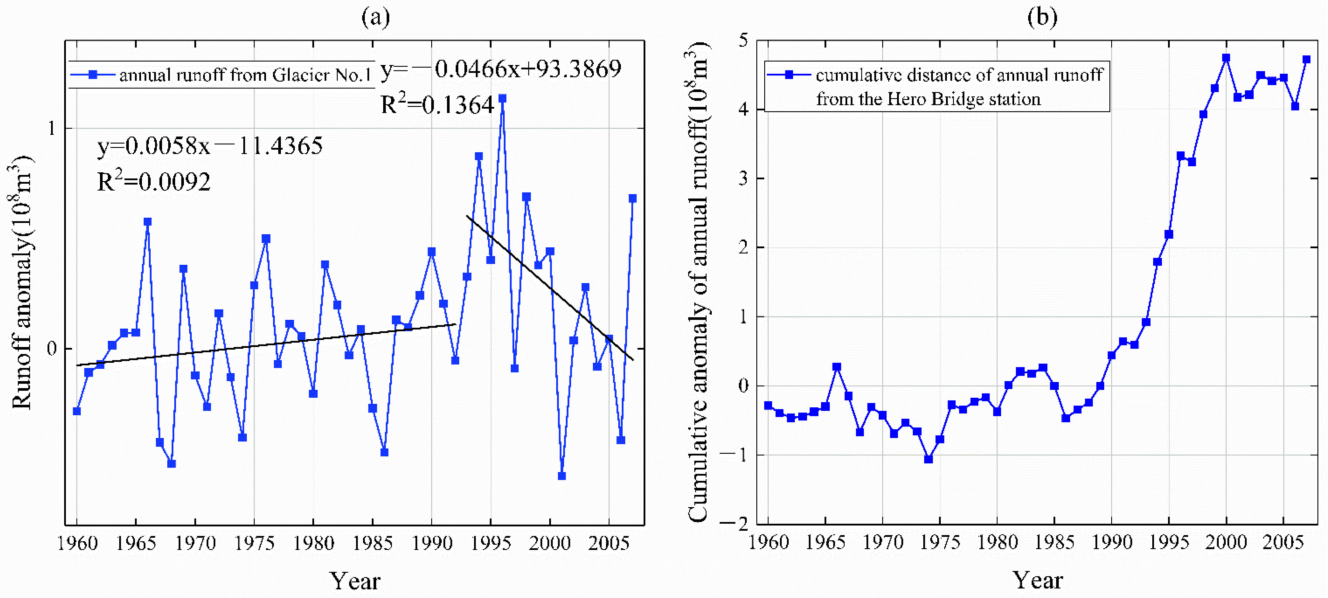


**Figure 11.** Runoff changes at the Hero Bridge hydrological station of the headwater region of the URB: (**a**) annual runoff, (**b**) cumulative anomaly of annual runoff, with the anomaly base period of 1960–1989.

## 4. Discussion

The annual temperature in northwest China showed a significant warming trend at a rate of 0.26 °C/decade from 1960 to 2019 [40], which is higher than the same period warming rate in all of China (0.23 °C/decade) [41]. In the Tian Shan Mountains, the response to global change is more sensitive [42]. Li et al. found that the overall warming trend in the Tian Shan region in 1961–2017 was 0.308 °C/decade [43], which is lower than the warming rate in the URB (0.362 °C/decade). Xu et al. analyzed meteorological data from 20 stations in the Tian Shan region from 1960 to 2016 and concluded that EDW exists only in summer in the Tian Shan region, with spring, autumn, winter, and annual warming trends showing a slight negative correlation with elevation [44]. The warming rate in the URB is faster than the increasing trend in the whole Tian Shan region, especially after 1990, when the warming was more significant, which is consistent with the results of others [45]. There are significant elevation differences in the warming rates in the Urumqi River Basin, which are 0.357 °C/decade, 0.360 °C/decade, 0.361 °C/decade, 0.362 °C/decade, 0.362 °C/decade, and 0.362 °C/decade. This indicates that there is elevation-dependent warming in the URB, but there are obvious seasonal differences, with increasing rates of change with increasing elevation in summer, autumn, and winter but not in spring.

Temperature and precipitation are key factors influencing glacier change [46], with precipitation determining glacier accumulation and temperature determining glacier ablation [47]. In the context of global warming, the accelerated retreat of glaciers in the Tian Shan [48] has become more sensitive to changes in temperature. Although precipitation increased during the same period, the contribution of increased precipitation to runoff could no longer compensate for the negative effects of increasing temperatures [49]. Wang et al. calculated the area change of approximately 3000 glaciers in each basin of the Tian Shan region from 1960 to 2009 and found that the area of the Tian Shan glaciers has shrunk by 11.5% in the last 50 years [50]. Changes in glacier area in the URB are related to climatic conditions and glacier size, but warming is the main cause of accelerated glacier melt in the URB. The rate of glacier retreat on the southern slopes of the URB is greater than that on the northern slopes due to the receipt of solar radiation and topographic differences. Over the past 58 years, the area of glaciers in the URB has shrunk by 57.8%, much higher

than the rate of retreat for the entire Tian Shan Mountains. The sensitivity of glaciers to climate change varies among different sizes. The smaller the area of the glaciers, the more sensitive they are to climate change, and high values of average annual retreat rates are often observed in smaller glacier areas in the Tian Shan Mountains [51]. The glaciers within the URB are small, with the largest individual glaciers not exceeding 5 $km^2$ in area, so glacier retreat in the URB is much higher than in the whole Tian Shan region. In this study, uncertainty calculations of 0.002 $km^2$ and 0.01 $km^2$ for individual glacier areas can be used for glacier analysis studies in the study area in comparison to other study cases for glacier uncertainty areas (Table 5). The advantage of this study compared to past studies [52] is that it not only studies glacier change, but also analyzes the impact of glacier changes on runoff with the background of EDW.

**Table 5.** Summary of relevant literature on glacier area based on remote sensing images in the Tian Shan Mountains.

| Study Area | Images Sources | Resolution | Mean Errors | References |
|---|---|---|---|---|
| Tomur Peak | Landsat ETM+ | 15 m | ±0.002 $km^2$ | Huai et.al., 2015 [53] |
| Aksu River basin | Landsat MSS/TM/ETM+/OLI | 79 m/30 m/15 m | ±0.5 pixel | Zhang et.al., 2019 [54] |
| Hala Lake Basin | Landsat MSS/TM/ETM+/OLI | 79 m/30 m/15 m | - | Li et.al., 2019 [55] |
| Urumqi River Basin | SPOT5<br>Landsat ETM+ | 5 m/15 m | ±0.003 $km^2$<br>±0.0001 $km^2$ | Huai et.al., 2018 [52] |
| Karatal river basin | Landsat TM/ETM+ | 30 m/15 m | <5% | Azamat et al., 2016 [56] |
| Tian Shan | Landsat TM/ETM+ | 30 m/15 m | <6% | Huai et al., 2017 [57] |
| Tian Shan | Landsat TM<br>Sentinel-2<br>Hexagon | 30 m/10 m/20 m | <2.6%<br><1.9%<br><2.9% | Li et.al., 2020 [58] |
| Urumqi River Basin | Landsat TM/ETM+/OLI | 30 m/15 m | ±0.002 $km^2$<br>±0.01 $km^2$ | This study |

There is a lag in the effect of climate warming on glacier change, and the length of this lag period is mainly determined by the size of the glacier [59]. Wang et al. suggested that the changes in mountain glaciers in the Northern Hemisphere lag climate change by approximately 12–13 a [60]. In this study, the abrupt change in temperature in the URB occurred in 1990, whereas the abrupt change in mass balance of Urumqi Glacier No. 1 occurred in 1993. Therefore, the glacier changes in response to temperature change lags 3 years in the URB.

Glacial meltwater is an important factor in the change in total runoff in the URB. From 1960 to 1996, glacier storage decreased by 33.4% (Table 4), generating runoff of approximately 26.9 × $10^8$ $m^3$, which accounted for 30.1% of the total runoff in the URB in this period. From 1996 to 2006, glacier storage decreased by 29.1%, and it generated runoff of approximately 15.6 × $10^8$ $m^3$, which accounted for 51.1% of the total runoff during this period. Thus, glacial storage has decreased dramatically, and the contribution of glacial meltwater runoff to the total runoff has increased since 1990.

Global warming leads to increased river runoff affected by glacier replenishment. By analyzing the changes in glacier mass balance, Zemp et al. believed that from 1961 to 2016, the mass loss of glaciers worldwide was severe. The contribution rate of glacier meltwater to sea level rise reached 25% to 30% [61]. It is expected that glacier retreat and mass loss will continue throughout the 21st century [62,63]. Huss et al. simulated and calculated the glacier runoff changes in 56 glacier cover basins in the world through the model and analyzed the influence of glacier changes on runoff. The simulation results showed that about half of the glacier runoff in the basin would continue to rise, and there would be a steady downward trend after reaching the peak [64]. With the background of global warming, with the decrease of glacier area, glacier meltwater would inevitably decrease in a certain period, called the inflection point of glacier runoff [65]. Based on the observation data of the Tian Shan glacier observation experimental station from 1959 to

2017, the runoff of No. 1 Glacier Basin in URB has showed a ladder-shaped increase since 1992, which was related to the significant increase of precipitation and temperature [31]. Glacier runoff in the URB will show a decreasing trend in approximately 2050 [66]. The temperature rise accelerates the melting and retreat of glaciers in mountainous areas, changes the composition of water resources, and intensifies the volatility and uncertainty of water resources.

The Urumqi River is an important source of water resources for the downstream region. The trend of glacier runoff in the URB is broadly similar to the trend of temperature in the basin. Rising temperatures and increased glacial meltwater were important causes of the total runoff increase in the Urumqi River until 1996, accounting for 30% of the total runoff from the 1960s to 1996. The total runoff in the URB is influenced not only by glacier melt but also by snowmelt and precipitation (especially precipitation in the high mountainous areas), which together determine the magnitude of total runoff [67].

## 5. Conclusions

The headwater region of the URB warmed significantly from 1960 to 2017, with a warming rate of 0.362 °C/decade, and an abrupt change occurred around 1990. At the same time, the warming rate increased with elevation in the URB. The elevation-dependent warming is distinctly seasonal, with the most pronounced warming in summer, autumn, and winter, and the least pronounced warming in spring.

The retreat of glaciers has accelerated under regional warming in the headwater region of the URB. The decreasing rate of glacier area reached 10%/decade, especially in the middle- and low-elevation regions. The cumulative anomaly of mass balance in Urumqi Glacier No. 1 reached −19,572 mm w. e. from 1960 to 2017, which indicates that Urumqi Glacier No. 1 thinned by 19.572 m. The mass balance and glacier meltwater runoff of Urumqi Glacier No. 1 experienced an abrupt change around 1993. This indicates that there is a lag of 3 years in the response of glacier changes to temperature in the headwater region of the URB. Elevation-dependent warming has a significant influence on glacier changes ($R^2$ = 0.49), especially in areas below 4000 m above sea level.

Glacial meltwater is an important factor in the change in total runoff in the headwater region of the URB. From 1960 to 1996, runoff showed an increasing trend ($5.8 \times 10^5$ $m^3$/a), and glacial meltwater accounted for 33.4% of the total runoff, whereas runoff showed a decreasing trend of $-4.6 \times 10^6$ $m^3$ from 1996 to 2007.

**Author Contributions:** Conceptualization, Z.Z., H.D. and Z.L.; methodology, Z.Z. and S.H.; software, S.J., Y.C. and M.L.; validation, Y.C. and P.L.; formal analysis, H.D. and L.G.; investigation, S.H., S.J. and P.L.; data curation, Z.L. and S.J.; writing—original draft preparation, Z.Z.; writing—review and editing, S.H., H.D. and Z.L.; visualization, Z.Z., X.C., L.G. and M.L.; supervision, H.D.; project administration, H.D.; funding acquisition, H.D. All authors have read and agreed to the published version of the manuscript.

**Funding:** This work was supported by the Projects for National Natural Science Foundation of China (41807159).

**Institutional Review Board Statement:** Not applicable.

**Informed Consent Statement:** Not applicable.

**Data Availability Statement:** Not applicable.

**Acknowledgments:** Thanks for the data support provided by the National Platform for Basic Conditions of Science and Technology—the National Earth System Science Data Center, the United States Geological Survey provided Landsat remote sensing image data, and the United States Space Administration provided digital elevation data. The authors appreciate the comments and encouragement given by the reviewers, editor, and associate editor.

**Conflicts of Interest:** The authors declare no conflict of interest.

## References


1. Alexander, L.; Allen, S.; Bindoff, N.L. *Climate Change 2013: The Physical Science Basis—Summary for Policymakers*; Intergovernmental Panel on Climate Change: Geneva, Switzerland, 2013. [CrossRef]
2. Barry, R.G. The status of research on glaciers and global glacier recession: A review. *Prog. Phys. Geogr.* **2006**, *30*, 285–306. [CrossRef]
3. Kraaijenbrink, P.D.A.; Stigter, E.E.; Yao, T.; Immerzeel, W.W. Climate change decisive for Asia's snow meltwater supply. *Nat. Clim. Change* **2021**, *11*, 591–597. [CrossRef]
4. Wang, S.; Zhao, X.; Guo, D.; Huang, Y. Response of permafrost to climate change in the Qinghai-Xizang plateau. *J. Glaciol. Geocryol.* **1996**, *18*, 157–165.
5. Zhu, L.; Xu, S.; Chen, P. Study on the impact of land use/land cover change on soil erosion in mountainous areas. *Geogr. Res.* **2003**, *22*, 432–438. [CrossRef]
6. Beniston, M. Climatic change in mountain regions: A review of possible impacts. *Clim. Change* **2003**, *59*, 5–31. [CrossRef]
7. Krasting, J.P.; Broccoli, A.J.; Dixon, K.W.; Lanzante, J.R. Future changes in northern hemisphere snowfall. *J. Clim.* **2013**, *26*, 7813–7828. [CrossRef]
8. Dariane, A.B.; Khoramian, A.; Santi, E. Investigating spatiotemporal snow cover variability via cloud-free MODIS snow cover product in Central Alborz Region. *Remote Sens. Environ.* **2017**, *202*, 152–165. [CrossRef]
9. Benn, D.I.; Bolch, T.; Hands, K.; Gulley, J.; Luckman, A.; Nicholson, L.I.; Quincey, D.; Thompson, S.; Toumi, R.; Wiseman, S. Response of debris-covered glaciers in the Mount Everest region to recent warming, and implications for outburst flood hazards. *Earth-Sci. Rev.* **2012**, *114*, 156–174. [CrossRef]
10. Lutz, A.F.; Immerzeel, W.W.; Shrestha, A.B.; Bierkens, M.F.P. Consistent increase in High Asia's runoff due to increasing glacier melt and precipitation. *Nat. Clim. Change* **2014**, *4*, 587–592. [CrossRef]
11. Luo, P.; Mu, Y.; Wang, S.; Zhu, W.; Mishra, B.K.; Huo, A.; Zhou, M.; Lyu, J.; Hu, M.; Duan, W.; et al. Exploring sustainable solutions for the water environment in Chinese and Southeast Asian cities. *Ambio* **2021**, *51*, 1199–1218. [CrossRef]
12. Pepin, N.; Bradley, R.S.; Diaz, H.F.; Baraer, M.; Caceres, E.B.; Forsythe, N.; Fowler, H.; Greenwood, G.; Hashmi, M.Z.; Liu, X.D.; et al. Elevation-dependent warming in mountain regions of the world. *Nat. Clim. Change* **2015**, *5*, 424–430. [CrossRef]
13. Vuille, M.; Bradley, R.S. Mean annual temperature trends and their vertical structure in the tropical Andes. *Geophys. Res. Lett.* **2000**, *27*, 3885–3888. [CrossRef]
14. Beniston, M.; Rebetez, M. Regional behavior of minimum temperatures in Switzerland for the period 1979–1993. *Theor. Appl. Climatol.* **1996**, *53*, 231–243. [CrossRef]
15. Minder, J.R.; Letcher, T.W.; Liu, C. The character and causes of elevation-dependent warming in high-resolution simulations of rocky mountain climate change. *J. Clim.* **2018**, *31*, 2093–2113. [CrossRef]
16. Williamson, S.N.; Zdanowicz, C.; Anslow, F.S.; Clarke, G.K.C.; Copland, L.; Danby, R.K.; Flowers, G.E.; Holdsworth, G.; Jarosch, A.H.; Hik, D.S. Evidence for elevation-dependent warming in the St. Elias Mountains, Yukon, Canada. *J. Clim.* **2020**, *33*, 3253–3269. [CrossRef]
17. Deng, H.; Chen, Y. Influences of recent climate change and human activities on water storage variations in Central Asia. *J. Hydrol.* **2017**, *544*, 46–57. [CrossRef]
18. Pepin, N.; Deng, H.; Zhang, H.; Zhang, F.; Kang, S.; Yao, T. An examination of temperature trends at high elevations across the Tibetan plateau: The use of MODIS LST to understand patterns of elevation-dependent warming. *J. Geophys. Res.-Atmos.* **2019**, *124*, 5738–5756. [CrossRef]
19. Deng, H.; Chen, Y.; Wang, H.; Zhang, S. Climate change with elevation and its potential impact on water resources in the Tianshan Mountains, Central Asia. *Glob. Planet Change* **2015**, *135*, 28–37. [CrossRef]
20. Gao, L.; Deng, H.; Lei, X.; Wei, J.; Chen, Y.; Li, Z.; Ma, M.; Chen, X.; Chen, Y.; Liu, M.; et al. Evidence of elevation-dependent warming from the Chinese Tian Shan. *Cryosphere* **2021**, *15*, 5765–5783. [CrossRef]
21. Shi, Y. Estimation of the water resources affected by climatic warming and glacier shrinkage before 2050 in West China. *J. Glaciol. Geocryol.* **2012**, *23*, 333–341. [CrossRef]
22. Liu, S.; Yao, X.; Guo, W.; Xu, J.; Shang Guan, D.; Wei, J.; Bao, W.; Wu, L. The contemporary glaciers in China based on the Second Chinese Glacier Inventory. *Acta Geogr. Sin.* **2015**, *70*, 3–16. [CrossRef]
23. Yang, X.; Han, T. The variation trends of temperature and precipitation and their influence on glaciers in the headwaters of the Urumqi River. *J. Glaciol. Geocryol.* **2012**, *18*, 189–193.
24. Li, H.; Wang, P. Research on the changes of the Urumqi Glacier No. 1, Tianshan Mountains based on multi-source remote sensing data. *J. Glaciol. Geocryol.* **2021**, *43*, 1018–1026. [CrossRef]
25. Wang, P.; Li, Z.; Zhou, P.; Li, H.; Yu, G.; Xu, C.; Wang, L. Long-term change in ice velocity of Urumqi Glacier No. 1, Tian Shan, China. *Cold Reg. Sci. Tech.* **2018**, *145*, 177–184. [CrossRef]
26. Sun, M.; Li, Z.; Yao, X.; Jin, S. Rapid shrinkage and hydrological response of a typical continental glacier in the arid region of northwest China—Taking Urumqi Glacier No.1 as an example. *Ecohydrology* **2013**, *6*, 909–916. [CrossRef]
27. XiangYing, L.; YongJian, D.; BaiSheng, Y.; TianDing, H. Changes in physical features of Glacier No. 1 of the Tianshan Mountains in response to climate change. *Chin. Sci. Bull.* **2011**, *56*, 2820–2827. [CrossRef]
28. Li, X. *Urumqi River Basin Journal*; Xinjiang People's Publishing House: Xinjiang, China, 2000; ISBN 7-228-05739-2.
29. Zhang, R. Urumqi River water resources evaluation study. *Water Conserv. Sci. Technol. Econ.* **2010**, *16*, 179–182. [CrossRef]

30. Wu, S.; Liu, Z.; Han, P.; Zhu, Y. Impact of climate change on water resources of the Ürüqi River basin. *J. Glaciol. Geocryol.* **2012**, *28*, 703–706. [CrossRef]
31. Jia, Y.; Li, Z.; Jin, S.; Xu, C.; Deng, H.; Zhang, M. Runoff changes from Urumqi Glacier No. 1 over the past 60 years, Eastern Tianshan, Central Asia. *Water* **2020**, *12*, 1286. [CrossRef]
32. Veettil, B.K.; Bremer, U.F.; Grondona, A.E.B.; De Souza, S.F. Recent changes occurred in the terminus of the Debriscovered Bilafond Glacier in the Karakoram Himalayas using remotely sensed images and digital elevation models (1978–2011). *J. Mt. Sci.* **2014**, *11*, 398–406. [CrossRef]
33. Pope, A.; Rees, G. Using in situ spectra to explore Landsat classification of glacier surfaces. *Int. J. Appl. Earth Obs.* **2014**, *27*, 42–52. [CrossRef]
34. Guo, W.; Liu, S.; Xu, J.; Wei, J.; Ding, L. Monitoring recent surging of the Yulinchuan Glacier on North Slopes of Muztag Range by remote sensing. *J. Glaciol. Geocryol.* **2012**, *34*, 765–774.
35. Hall, D.K.; Bayr, K.J.; Schöner, W.; Bindschadler, R.A.; Chien, J.Y.L. Consideration of the errors inherent in mapping historical glacier positions in Austria from the ground and space (1893–2001). *Remote Sens. Environ.* **2003**, *86*, 566–577. [CrossRef]
36. Liu, S.Y.; Sun, W.X.; Shen, Y.P.; Li, G. Glacier changes since the Little Ice Age maximum in the western Qilian Shan, northwest China, and consequences of glacier runoff for water supply. *J. Glaciol.* **2003**, *49*, 117–124. [CrossRef]
37. Burn, D.H.; Elnur, M.a.H. Detection of hydrologic trends and variability. *J. Hydrol.* **2002**, *255*, 107–122. [CrossRef]
38. Sen, K.P. Estimates of the regression coefficient based on Kendall's Tau. *Publ. Am. Stat. Assoc.* **1968**, *63*, 1379–1389. [CrossRef]
39. Huang, J.; Chen, W.; Wen, Z.; Zhang, G.; Li, Z.; Zuo, Z.; Zhao, Q. Chinese atmospheric science research since the founding of New China 70 years ago: Climate and climate change Climate Change. *Sci. Sin.-Terrae* **2019**, *49*, 1607–1640. [CrossRef]
40. Li, Z.; Ding, Y.; Chen, A.; Zhang, Z.; Zhang, S. Characteristics of warming hiatus of the climate change in Northwest China from 1960 to 2019. *Acta Geogr. Sin.* **2020**, *75*, 1845–1859. [CrossRef]
41. Alexander, L.; Allen, S.; Bindoff, N.; Breon, F.-M.; Church, J.; Cubasch, U.; Emori, S.; Forster, P.; Friedlingstein, P.; Gillett, N.; et al. Climate change 2013: The physical science basis, in contribution of Working Group I (WGI) to the Fifth Assessment Report (AR5) of the Intergovernmental Panel on Climate Change (IPCC). In *Climate Change 2013: The Physical Science Basis*; Intergovernmental Panel on Climate Change: Geneva, Switzerland, 2013. [CrossRef]
42. Yao, J.; Yang, Q.; Liu, Z.; Li, C. Spatio-temporal change of precipitation in arid region of the Northwest China. *Acta Ecol. Sin.* **2015**, *35*, 5846–5855. [CrossRef]
43. Li, B.; Chen, Y.; Shi, X. Does elevation dependent warming exist in high mountain Asia? *Environ. Res. Lett.* **2020**, *15*, 024012. [CrossRef]
44. Xu, M.; Kang, S.; Wu, H.; Yuan, X. Detection of spatio-temporal variability of air temperature and precipitation based on long-term meteorological station observations over Tianshan Mountains, Central Asia. *Atmos. Res.* **2018**, *203*, 141–163. [CrossRef]
45. Li, R.; Zhang, M.; Jin, S.; Xiong, Y.; Liu, Y. Regional difference and catastrophe of climate change over Urumqi River Basin. *Acta Geogr. Sin.* **2010**, *33*, 243–250. [CrossRef]
46. Ali, I.; Shukla, A.; Romshoo, S.A. Assessing linkages between spatial facies changes and dimensional variations of glaciers in the upper Indus Basin, western Himalaya. *Geomorphology* **2017**, *284*, 115–129. [CrossRef]
47. Shi, Y. *Concise Catalogue of Chinese Glaciers*; Shanghai Popular Science Press: Shanghai, China, 2005.
48. Xu, L.; Li, P.; Li, Z.; Zhang, Z.; Wang, P.; Xu, C. Advances in research on changes and effects of glaciers in Xinjiang mountains. *Adv. Water Sci.* **2020**, *31*, 946–959. [CrossRef]
49. Liu, C.; Kang, E.; Liu, S.Y.; Chen, J.; Liu, Z. A study of glacier changes and their runoff effects in the Northwest Arid Zone. *Sci. China Ser. D* **1999**, *29*, 55–62. [CrossRef]
50. Wang, S.; Zhang, M.; Li, Z.; Wang, F.; Li, H.; Li, Y.; Huang, X. Response of glacier area variation to climate change in Chinese Tianshan Mountains in the past 50 years. *Acta Geogr. Sin.* **2011**, *66*, 38–46. [CrossRef]
51. Ye, B.; Ding, Y.; Liu, C. Response of valley glaciers in various size and their runoff to climate change. *J. Glaciol. Geocryol.* **2001**, *23*, 103–110. [CrossRef]
52. Huai, B.; Wang, Y.; Li, Z.; Sun, W.; Wang, X. Glacier changes and its effect on water resources in Urumqi River Basin, Tianshan Mountains, China, from 1964 to 2014. *Arab. J. Geosci.* **2018**, *11*, 716. [CrossRef]
53. Baojuan, H.; Zhongqin, L.; Meiping, S.; Wenbin, W.; Shang, J.; Kaiming, L. Change in glacier area and thickness in the Tomur Peak, western Chinese Tien Shan over the past four decades. *J. Earth Syst. Sci.* **2015**, *124*, 353–363. [CrossRef]
54. Zhang, Q.; Chen, Y.; Li, Z.; Li, Y.; Xiang, Y.; Bian, W. Glacier changes from 1975 to 2016 in the Aksu River Basin, Central Tianshan Mountains. *J. Geogr. Sci.* **2019**, *29*, 984–1000. [CrossRef]
55. Li, D.-S.; Cui, B.-L.; Wang, Y.; Xiao, B.; Jiang, B.-F. Glacier extent changes and possible causes in the Hala Lake Basin of Qinghai-Tibet Plateau. *J. Mt. Sci.* **2019**, *16*, 1571–1583. [CrossRef]
56. Kaldybayev, A.; Chen, Y.; Vilesov, E. Glacier change in the Karatal river basin, Zhetysu (Dzhungar) Alatau, Kazakhstan. *Ann. Glaciol.* **2016**, *57*, 11–19. [CrossRef]
57. Baojuan, H.; Weijun, S.; Yetang, W.; Zhongqin, L. Glacier shrinkage in the Chinese Tien Shan Mountains from 1959/1972 to 2010/2012. *Arct. Antarct. Alp. Res.* **2017**, *49*, 213–225. [CrossRef]
58. Li, Y. Glacier changes and their linkage to the climate-topographic context in the Borohoro Mountains, Tian Shan 1977–2018. *Water* **2020**, *12*, 1502. [CrossRef]

59. Ren, J.; Qing, D.; Kang, S.; Hou, S.; Pu, J.; Jin, Z. Characteristics of glacial change and climatic warming and drying in the Central Himalayas. *Chin. Sci. Bull.* **2003**, *48*, 2478–2482. [CrossRef]
60. Wang, N.; Zhang, X. Mountain glacier fluctuations and climatic change during the last 100 years. *J. Glaciol. Geocryol.* **1992**, *14*, 242–250.
61. Zemp, M.; Huss, M.; Thibert, E.; Eckert, N.; McNabb, R.; Huber, J.; Barandun, M.; Machguth, H.; Nussbaumer, S.U.; Gärtner-Roer, I.; et al. Global glacier mass changes and their contributions to sea-level rise from 1961 to 2016. *Nature* **2019**, *568*, 382–386. [CrossRef]
62. Huss, M.; Hock, R. A new model for global glacier change and sea-level rise. *Front. Earth Sci.* **2015**, *3*, 54. [CrossRef]
63. Marzeion, B.; Jarosch, A.H.; Hofer, M. Past and future sea-level change from the surface mass balance of glaciers. *Cryosphere* **2012**, *6*, 1295–1322. [CrossRef]
64. Farinotti, D.; Huss, M.; Fürst, J.J.; Landmann, J.; Machguth, H.; Maussion, F.; Pandit, A. A consensus estimate for the ice thickness distribution of all glaciers on Earth. *Nat. Geosci.* **2019**, *12*, 168–173. [CrossRef]
65. Huss, M.; Hock, R. Global-scale hydrological response to future glacier mass loss. *Nat. Clim. Change* **2018**, *8*, 135–140. [CrossRef]
66. Xie, Z.; Wang, X.; Kang, E.; Feng, Q.; Li, Q.; Chen, L. Glacial runoff in China: An evaluation and prediction for the future 50 years. *J. Glaciol. Geocryol.* **2006**, *28*, 457–466.
67. Han, T.; Ye, B.; Ding, Y.; Jiao, K. Increasing runoff in the Ürüqi River Basin since 1980s. *J. Glaciol. Geocryol.* **2005**, *27*, 655–659.